

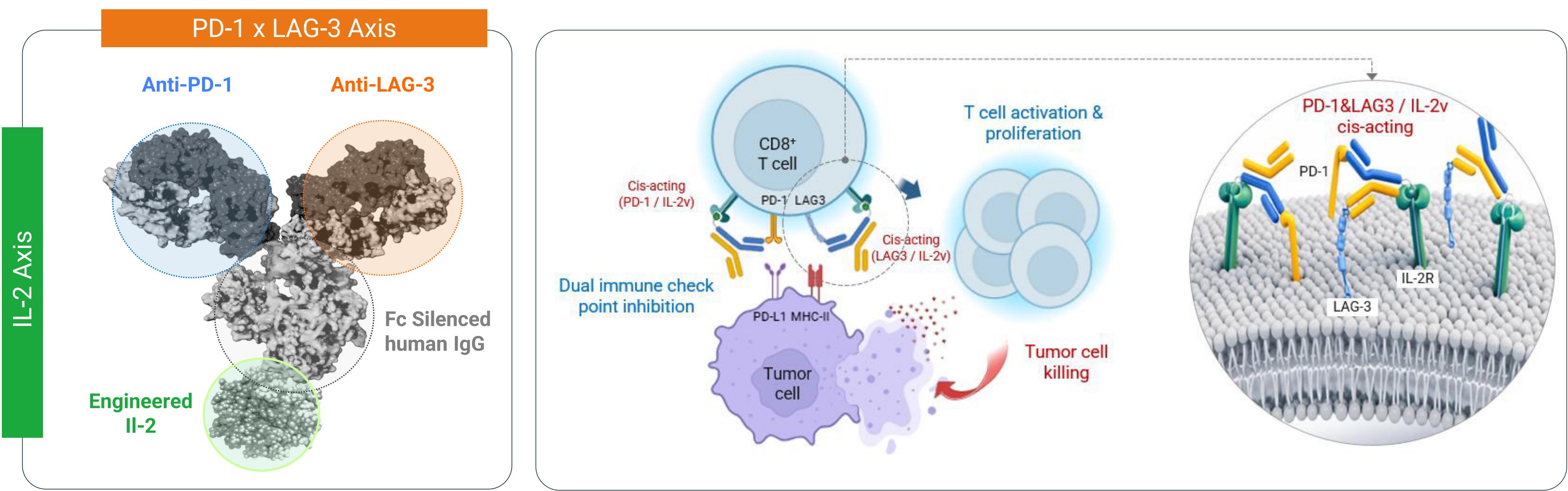
AR166, a First-in-Class PD-1xLAG-3xIL-2v Tri-specific Immunocytokine Delivering Cis-Acting IL-2v to Overcome Immune Checkpoint Inhibitor Resistance

Jaeho Song¹, Seon-mi Yu¹, Jae-Seok Lee¹, Jinkeol Mok¹, WooJeong Lee¹, Seo-Young Koo¹, Ye Rim Gu¹, Min-Young Park¹, Seoyun Yang¹, Young Woo Park¹, Wooick Jang¹, Su-Hyung Park², Juhan Yoon¹
¹Y-Biologics Inc. and ²Korea Advanced Institute of Science and Technology, Daejeon, Republic of Korea



Introduction

Immunocytokines fusing anti-PD-1 antibody with interleukin-2 (IL-2) have demonstrated therapeutic potential in clinical settings in overcoming resistance to PD-(L)1 inhibitors. However, clinical response rates were varied, highlighting the need for improved efficacy, particularly in tumors with primary and acquired resistance to PD-1 blockade expressing high levels of LAG-3. Emerging evidence indicates LAG-3, a key immune checkpoint, acts synergistically with PD-1 to promote T cell exhaustion, while dual blockade of LAG-3 and PD-1 can reprogram CD8⁺ T cells and Tregs to enhance antitumor immunity. Here, we present AR166, a novel tri-specific immunocytokine (“Multi-AbKine”) that simultaneously targets PD-1 and LAG-3 and incorporates an affinity-tuned IL-2 variant (IL-2v) to enable cis-acting immune stimulation.



AR166 demonstrates dual checkpoint blockade and complete Fc silencing

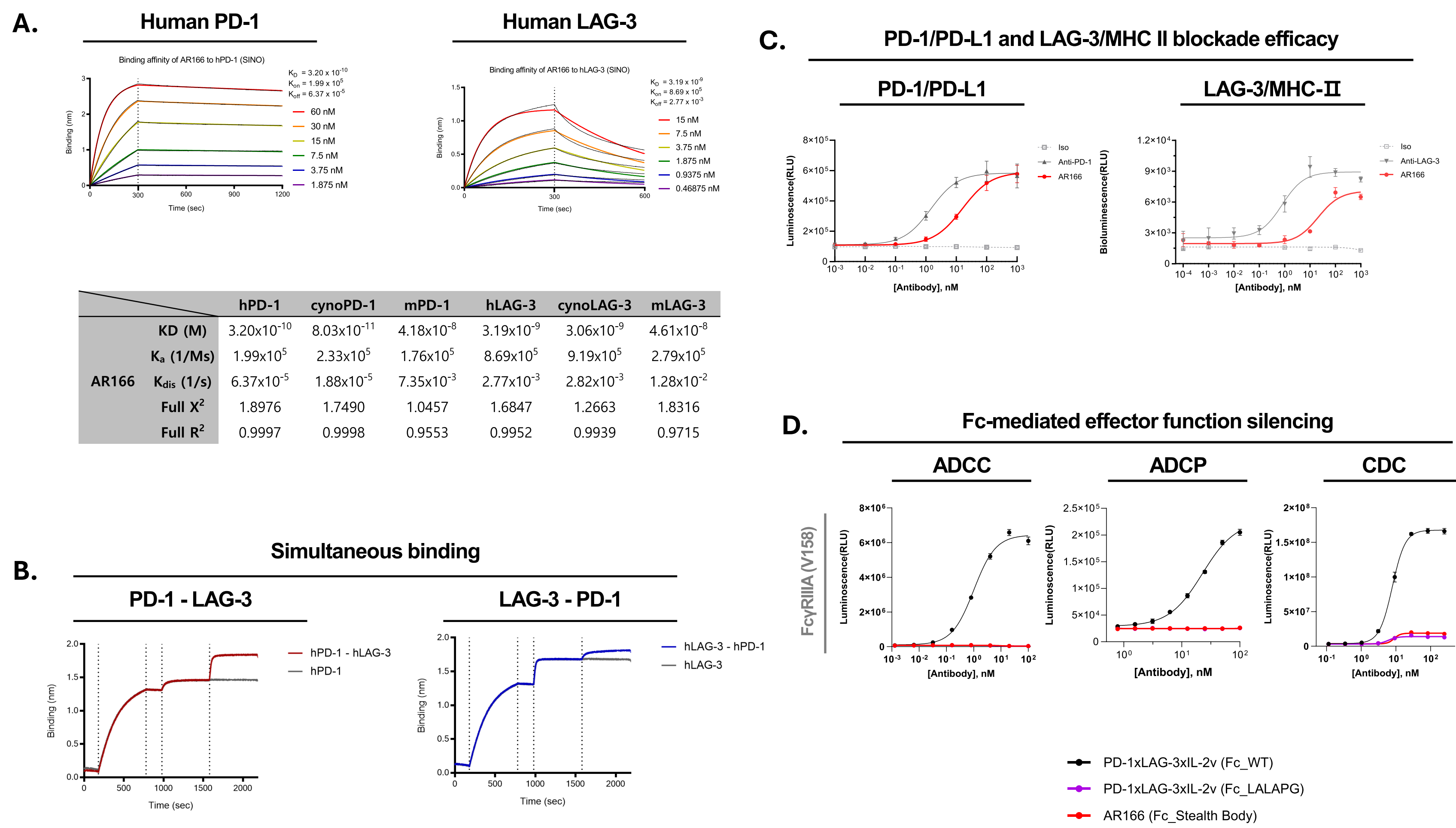


Figure 1. Target engagement, checkpoint blockade, and Fc silencing profile of AR166. (A) Binding kinetics of PD-1 and LAG-3 measured by BLI. (B) Simultaneous dual binding to PD-1 and LAG-3. (C) Blockade of PD-1/PD-L1 and LAG-3/MHC-II interactions. (D) Abolished Fc-mediated effector functions (ADCC, ADCP, CDC) comparable to LALAPG.

AR166 drives cis-acting IL-2v signaling through PD-1 and/or LAG-3 anchoring

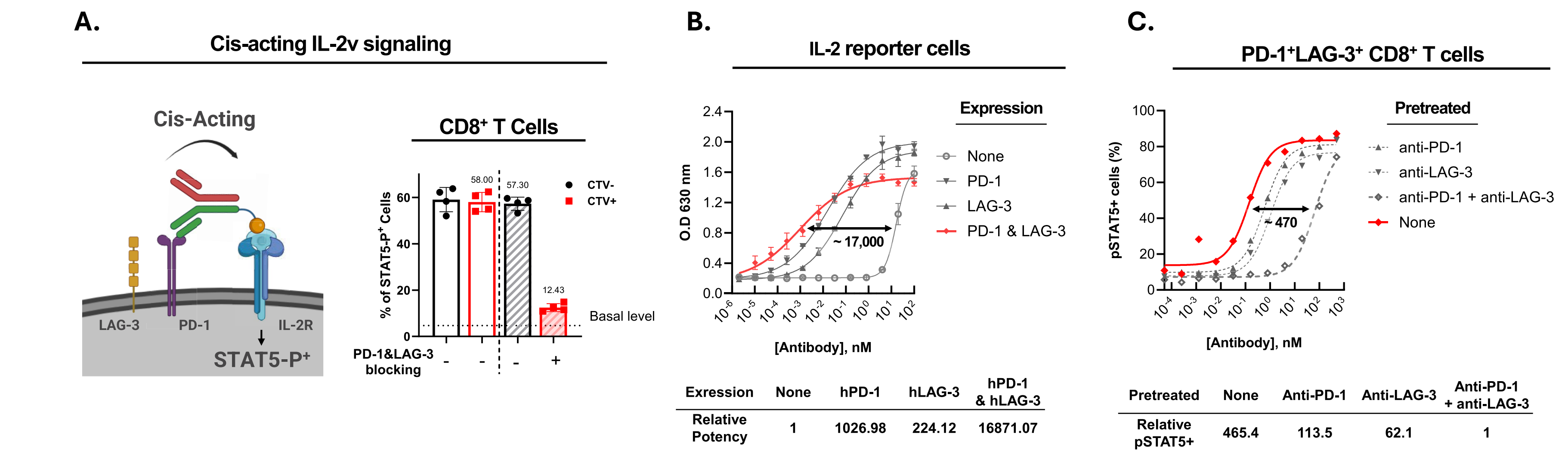


Figure 2. Cis-acting and target-anchored IL-2v activity of AR166. (A) Schematic and experimental validation of cis-acting, target-anchored IL-2v signaling. (left, schematic illustration; right, experimental comparison of cis- and trans-acting signaling.) (B) Target-dependent reporter activation (PD-1, LAG-3, or dual expression). (C) Differential pSTAT5 signaling upon target blockade in activated CD8⁺ T cells.

AR166 reinvigorates exhausted T cells induced by repeated activation and HCC patient-derived immune cells

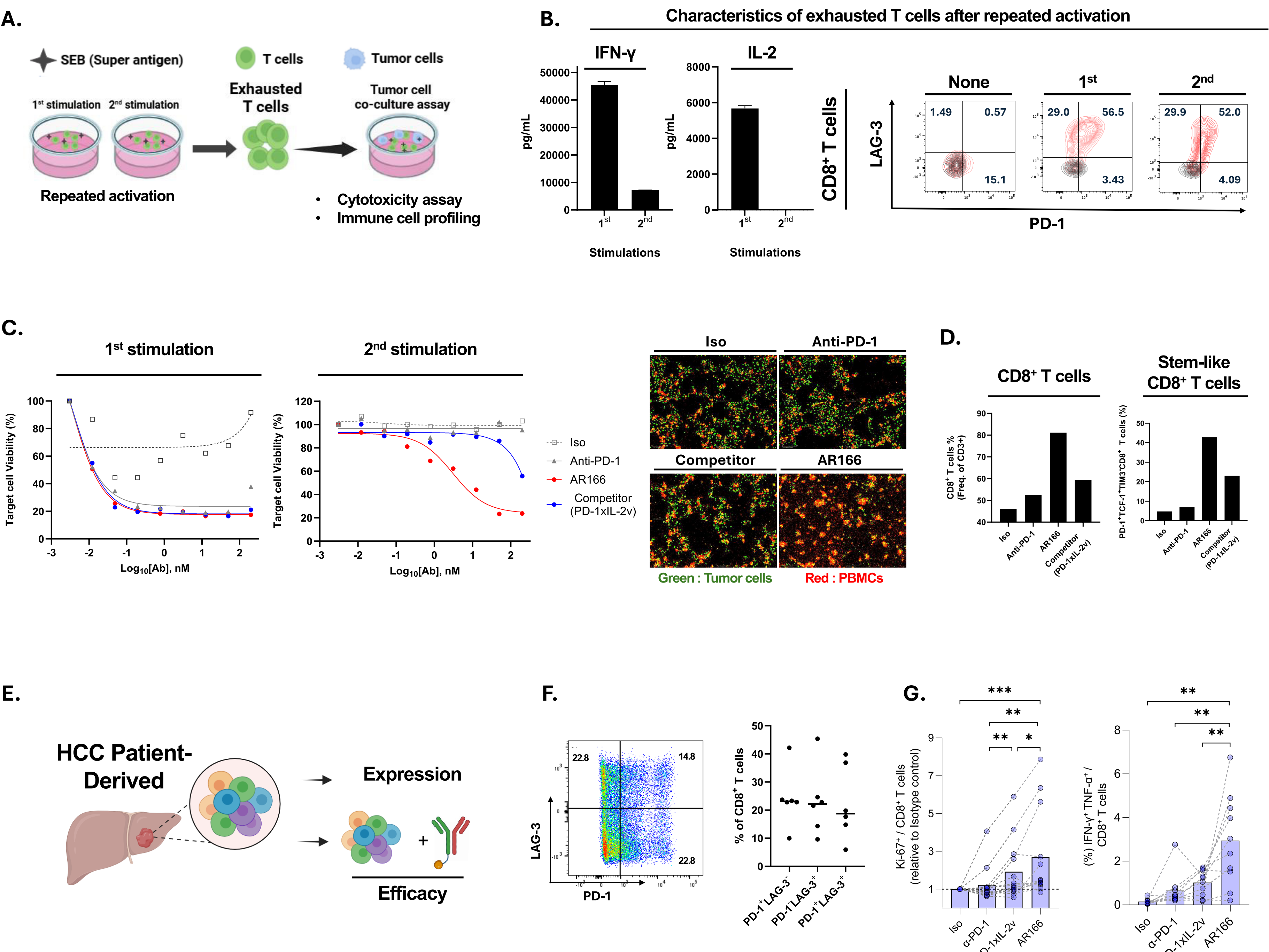


Figure 3. Effect of AR166 on cytotoxic activity and T cell function in a SEB-stimulated T cell exhaustion model (A-D) and HCC patient-derived samples (E-G). (A) Schematic of SEB-induced T cell exhaustion. (B) PD-1/LAG-3 expression and cytokine production (IFN-γ, IL-2) in CD8⁺ T cells following repeated stimulation with SEB. (C) Cytotoxicity in tumor cells co-cultured with repeatedly stimulated PBMCs (left, cytotoxicity assay; right, real-time luciferase imaging). (D) CD8⁺ and stem-like CD8⁺ T cell proliferation in tumor cells co-culture with repeatedly stimulated PBMCs. (E) Workflow for experiments using tumor-infiltrating immune cells from HCC patients. (F) A representative flow cytometry plot and summary data of PD-1 and LAG-3 expression on HCC patients-derived CD8⁺ T cells. (G) Evaluation of CD8⁺ T cell activation based on proliferation and IFN-γ/TNF-α production. Statistical analysis by Wilcoxon matched-pairs signed rank test; ***p<0.001, **p<0.01, *p<0.05.

AR166 induces stem-like CD8+ T cell expansion and durable antitumor immunity in anti-PD-1-resistant MC38 model

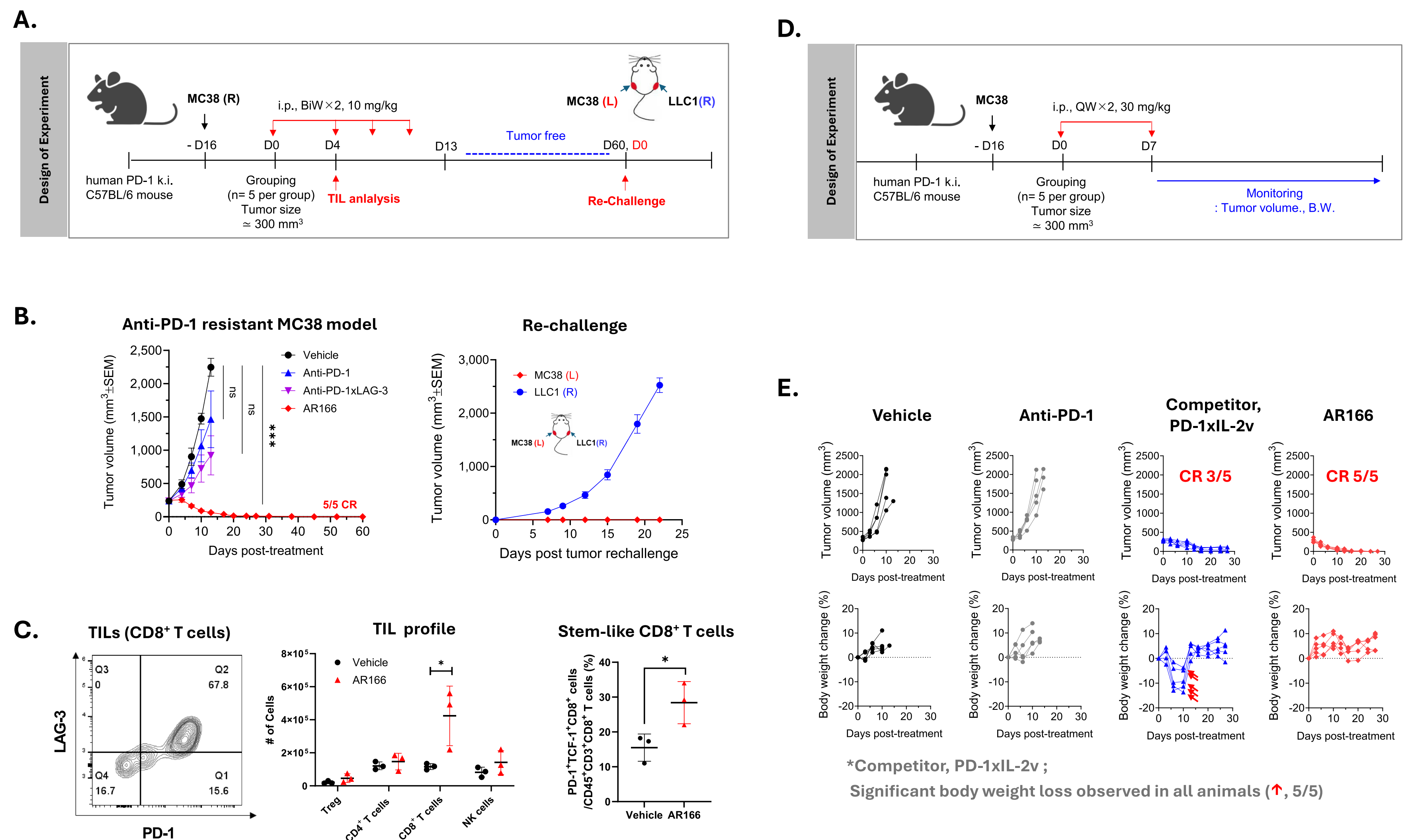


Figure 4. *In vivo* efficacy and mechanism of AR166 in an anti-PD-1-resistant MC38 mouse model. (A) Schematic of the anti-PD-1-resistant MC38 tumor model and experimental design for tumor cell re-challenge. (B) Tumor volume demonstrating resistance to anti-PD-1 treatment in the primary tumor setting (left) and re-challenge results showing sustained tumor control and immunological memory (right). Statistical analysis by Dunnett's one-way ANOVA; ***p<0.001. (C) PD-1 and LAG-3 expression in tumor-infiltrating CD8⁺ lymphocytes, with immune profiling demonstrating increased CD8⁺ and stem-like CD8⁺ T cell populations. Statistical analysis by Student's T test; *p<0.05. (D) Schematic of the treatment schedule for the anti-PD-1 resistant model. (E) Evaluation of tumor growth inhibition and body weight changes in MC38 syngeneic mice with acquired resistance to anti-PD-1 therapy.

AR166 demonstrates a favorable safety profile in cynomolgus monkeys

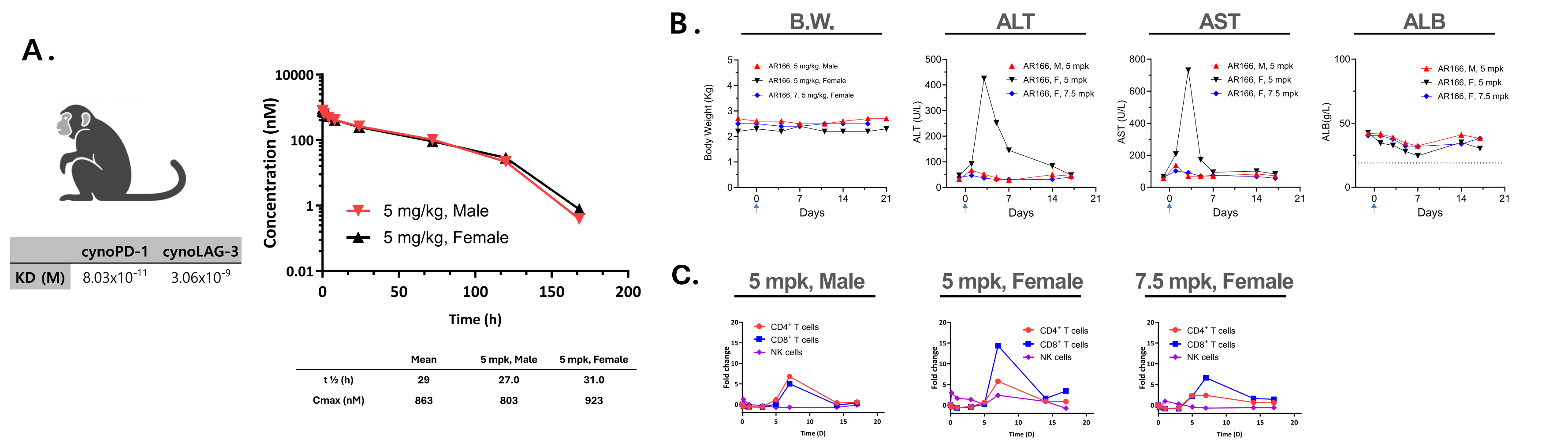


Figure 5. Pharmacokinetic and safety profile of AR166 in cynomolgus monkeys. (A) AR166 was administered as a single intravenous dose of 5 mg/kg. Serum concentrations were measured to generate concentration-time profiles, and pharmacokinetic parameters were derived by noncompartmental analysis. (B-C) Following administration of 5 and 7.5 mg/kg, body weight (B.W.), liver enzymes (ALT, AST), albumin (ALB), and peripheral immune cell profiling were evaluated. Study is ongoing.

Conclusion

Our findings show that AR166, a first-in-class PD-1xLAG-3xIL-2v tri-specific, can exceed the efficacy of both PD-1 inhibitors and PD-1xIL-2v with a favorable safety profile.